Pseudoelastic Deformation during Nanoscale Adhesive Contact Formation

Dan Mordehai, Eugen Rabkin, and David J. Srolovitz

Phys. Rev. Lett. **107**, 096101 — Published 23 August 2011

DOI: 10.1103/PhysRevLett.107.096101

Pseudoelastic Deformation During Nanoscale Adhesive Contact Formation

Dan Mordehai* and Eugen Rabkin
Department of Materials Engineering, Technion - Israel Institute of Technology, 32000 Haifa, Israel

David J. Srolovitz
Institute of High Performance Computing,1 Fusionopolis Way, 16-16 Connexis, Singapore 138632, Singapore.

Molecular dynamics simulations are employed to demonstrate that adhesive contact formation through classical jump-to-contact is mediated by extensive dislocation activity in metallic nanoparticles. The dislocations generated during jump-to-contact are completely annihilated by the completion of the adhesive contact, leaving the nanoparticles dislocation-free. This rapid and efficient jump-to-contact process is pseudoelastic, rather than purely elastic or plastic.

The growing interest in nanoscale structures for mechanical, electronic, and other novel applications has brought the control of nanomaterial synthesis and fabrication to the fore. Many synthesis methods depend sensitively on the nature of the adhesive contact between solids with characteristic dimensions in the nanometer range [1–3]. For example, adhesion is one of the central processes in the agglomeration and/or sintering of nanoparticles [4, 5]. Despite the obvious importance of an atomistic description of materials to nanoscale structures [6, 7], adhesion between solids is customarily described through macroscopic continuum models (typically of contact between elastically isotropic homogeneous bodies, with perfect, smooth, spherical, cylindrical or infinite-flat surfaces [8–10]). Most of these continuum models are based upon the assumption that the contacting bodies are elastic, whereas plastic deformation commonly occurs during adhesion [11, 12]. Kadin *et al.* [13] demonstrated that the stress which develops when a spherical particle jumps-to-contact may exceed the yield strength of the particles.

Nanoparticles, sythesized by many different routes (e.g. [14–16]), are commonly fully or partially faceted as a result of crystalline anisotropy in the surface energy and/or crystal growth rate (anisotropic shapes are more common on the nano- rather than bulk scale because the short atomic transport distances make achieving equilibrium or steady-state kinetic shapes easy). Yau and Thölén [17] experimentally demonstrated that faceted metallic particles establish adhesive contacts along their low-energy facets. Halder and Ravishankar [3] formed Au nanowires by adhesion of Au nanoparticles along their {111} facets. Interestingly, planar faults are often observed after nanoparticle adhesion; e.g., twin-boundaries and stacking faults were observed as a result of Au nanoparticle adhesion [3, 18]. Despite the fact that stacking faults were observed, no dislocations were identified within the nanoparticles during adhesive contact [3, 17, 18]. *A priori*, the absence of dislocations within the nanoparticles following contact would suggest that the resultant deformation is purely elastic. On the other hand, in molecular dynamics (MD) simulations reported in this letter, we show that even when parallel, atomically flat facets are brought into contact, very high local stresses develop as a result of adhesive forces and that these stresses are responsible for nucleation of dislocations. These dislocations are then rapidly cleared from the particles by the end of the adhesion process leaving pristine adhered nanoparticles in their wake.

Since Au is widely used in nanotechnology and in many nanoparticle studies and because of the availability of reliable many-body interatomic potentials for Au, we focus on Au nanoparticles in this study. Our simulations were performed using the interatomic potential of Grochola *et al.* [19], which yields good elastic properties and surface energies and was successfully employed to predict the strength of Au nanoparticles [20] (see Supplemental Materials in [21]). Our simulations were performed using the parallel, MD simulation code, LAMMPS [22]. We constructed faceted Au nanoparticles of equilibrium shape, as described by the Wulff construction [23] and the anisotropic surface energies for this interatomic potential (see [21]). Figure 1 shows the atomic configuration of a single faceted nanoparticle after MD relaxation. The atoms in the figure are shaded according to their absolute displacement from their perfect crystal locations to the relaxed positions. As reported recently by Huang *et al.* [24], there is an inhomogeneous relaxation of the surfaces and edges. The atoms along the edges, where facets meet, exhibit the largest displacement toward the particle center, as measured from the ideal face centered cubic (fcc) positions. These large inward displacements are the result of the forces associated with the discontinuity in the surface stress at the facet interfaces. These edge forces are balanced by stresses developed within the nanoparticles.

Two relaxed nanoparticles are joined along {111} facets. Stable, low energy, contact configurations can be established by joining the particles in a manner that retains the fcc packing along the contact surface or by rotating the two particles about the normal to the contact surface by $\pi/3$ to produce a perfect twin-boundary between them. Simple geometrical considerations demonstrate that in the second configuration, the

*Electronic address: danmord@tx.technion.ac.il

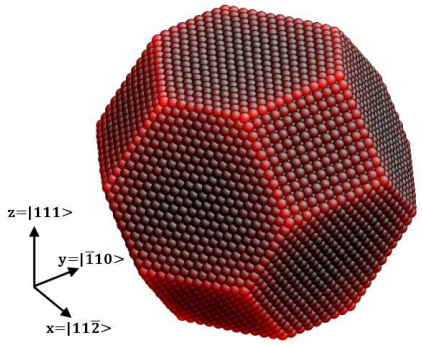

FIG. 1: (Color online) Relaxed atomic structure of a 7.4 nm Au nanoparticle. The shading of each atom indicates the magnitude of the displacements from the ideal face centered cubic lattice positions, toward the center of the particle (the brighter the atoms, the larger the displacement).

two hexagonal-shaped facets in the interface are in perfect coincidence, whereas in the first configuration the area of the interface is smaller than the facet area. Since the twin boundary energy is significantly smaller than the energy gain in {111} surface energy, the second configuration, with the twin boundary at the interface between the adhered particles, is energetically more favorable than the first (untwinned) one (the decrease in energy upon joining and relaxing two 5.7 nm particles in the twinned configuration is 7% larger than that in non-twinned case).

The simulations show that the facets do not stay flat while approaching one another. Before jumping into contact, the distance between the edges of the opposite facets is larger than the distance between their centers due to the convex shape of the relaxed facets. The facet centers first jump into contact, followed by the rest of the surface atoms; the contact wave spreads outward from the facet center. Figure 2 shows the distance between the facets along the $X = [11\overline{2} >$ axis, which passes through the center of the facet. Two additive processes contribute to the inhomogeneous deformation. First, because relaxed facets are convex, the atoms in the center of the facet are the first to interact with their counterparts from the approaching particle. The jump-to-contact wave that spreads across the facet can be regarded as an instability associated with "positive feedback," i.e., the approach of the facet centers leads to an increase in the attractive force, which in turn accelerates further approach. Second, the energy density of the elastic strain field generated by the adhesion forces between facets is not homogenously spread in the near-facet region due to the stress concentration at the edges and near the vertices. The tensile stresses acting on the atoms at the edges are higher than those in the middle of the facet. Thus, it requires more mechanical work to pull the atoms at the edges toward the approaching facet than it does for atoms in the facet center.

The particles undergo plastic deformation during the jump-to-contact. This occurs because of the large strains

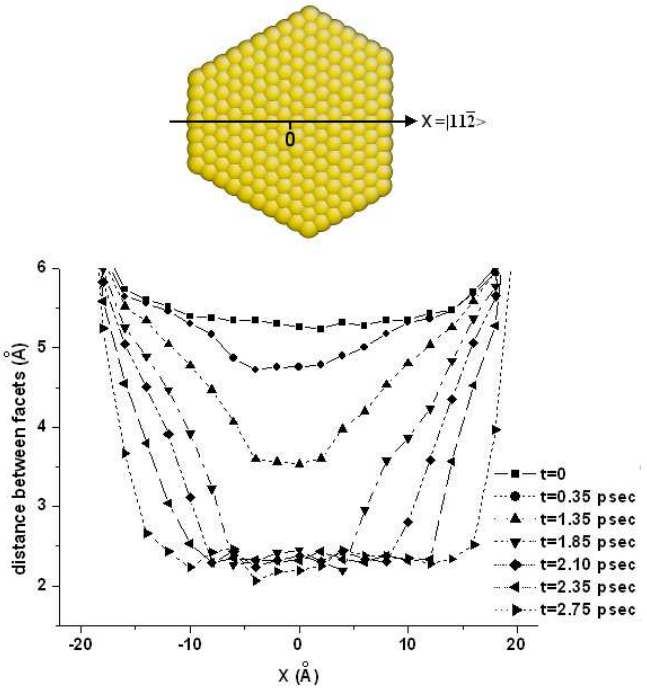

FIG. 2: (Color online) The distance between the adhering facets as a function of distance along the $X = [11\overline{2} >$ direction (see the upper image of the atomic structure of the facet). The plot shows this distance at several time steps during the jump-to-contact, considering $t = 0$ as the moment in which the jump-to-contact begins. The initial convex shape of the facet can be clearly identified.

that develop as the facets jump-to-contact and the inertias of the remainder of the two particles prevent them from keeping pace with the rapidly approaching facet centers. The inhomogeneous deformation produces local strain gradients along the jumping facet (see Fig. 2). The accompanying large elastic energies are relieved by nucleating dislocations. Shockley partial dislocations are nucleated at the surface on $(1\bar{1}1)$, $(\bar{1}11)$ and $(\overline{11}1)$ slip planes, glide into the particle interior, form sessile stair-rod dislocations and, if they glide far enough, meet at a single point to form a full stacking-fault tetrahedron (SFT), as illustrated in Fig. 3(a). Interestingly, the first partial dislocations do not form at the edges where facets meet, but rather nucleate closer to the center of the atomically flat facet [25, 26].

The SFTs are transient structures. After the facet-facet contact line advances by a short distance, the initial partial dislocation is followed by a partial dislocation of opposite sign (not a classical trailing partial) on the same slip plane that annihilates the stacking fault (see Fig. 3(b)). Since the net Burgers vector of this pair of partial dislocations is zero, no surface slip steps are formed and there is no permanent plastic deformation. At the same time, additional partial dislocations are emitted from the facet on slip planes adjacent to and parallel to those of the initial dislocations (Fig. 3(b)). This nucleation is

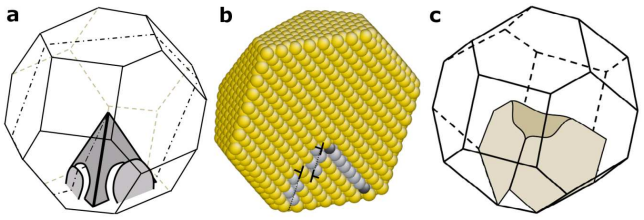

FIG. 3: (Color online) Dislocation activity during jump into contact. (a) A sketch of the dislocation structures formed inside a particle during contact formation (see text). The gray shaded areas represent stacking faults. (b) The atomic structure of the particle in the cross-section marked with the dotted line in (a). The atoms in the partial dislocation cores and stacking faults are shaded in gray, where the other (bulk and surface) atoms are in yellow. The gray atomic string on the right hand side represents the core of a stair-rod dislocation. (c) A sketch of the partial dislocations emitted from the edges between the nanoparticles {111} facet and the neighboring {100} facets.

actually a dislocation dipole nucleation event. The energy required to nucleate such a narrow dipole structure is small since it induces only a very short-range strain field in the nanoparticle. This process of partial dislocation and stacking fault formation, followed by nucleation of the opposite partial and stacking fault annihilation, occurs plane after plane as the contact line advances.

The nucleation process continues until the final partial dislocations are nucleated at the edges of the adhered facet and the adjacent {100} facets. While expanding into the crystal, these partial dislocations bow into the nanoparticle, but in all simulations of nanoparticle-nanoparticle contact, these dislocations did not bow far enough into the bulk to form a SFT and glissile segments remained at the top of the stacking faults (see Fig. 3(c)). As the atoms far from the contact region accelerate, these segments are pulled back towards the facet edges, leaving a defect-free particle at the end of the jump-to-contact. This is an important point: after the jump-to-contact process is complete, there are no dislocations in the particle, the particle surface has no slip steps, and the final particle shape is exactly the same as that of the original particle. This adhesion mechanism, in which dislocations are nucleated but no residual plastic deformation is left, is *pseudoelastic*. Visual example of the process described here-in is provided in a multimedia file in the Supplemental Materials in [21].

Similar behavior was identified when a faceted particle comes into adhesive contact with a semi-infinite substrate. When the nanoparticle approached the flat substrate, the interatomic forces pulls them into contact first at a single point. Due to the size difference between the adhering bodies, the particle accommodated most of the deformation. The adhesion zone spread from the point of contact outwards along the interface. During this process, dislocations are found to be nucleated only in the particle. Despite the large deformation, no dislocation debris was identified within either the nanoparticle or substrate after the completion of the adhesion process.

The present results demonstrate that significant dislocation activity occurs in faceted nanoparticles during the formation of adhesive contacts. The simulations also show that after the contact forms, the nanoparticles fully recover their initial, defect-free state. The dislocation activity accommodates the large elastic strains that develop in the contact zone *during* jump-to-contact.

This pseudoelastic mechanism is energetically more favorable than fully elastic jump to contact, as seen in the plot of energy change versus the macroscopic reaction coordinate (distance between the centers of mass of the particles) in Fig. 4. The reaction coordinate describes the normalized distance between the centers of the particles during the MD simulation. In particular, the final state is the minimum energy configuration after contact is formed. In order to calculate the energy gain along a trajectory in phase space corresponding to a fully elastic jump to contact, we performed energy minimization perpendicular to the reaction coordinate (via conjugate gradient) on a series of atomic configurations which continuously connect the initial and final states. The "elastic" curve in Fig. 4 corresponds to the energy change of the relaxed atomic configuration of the particles as the particle centers are stepped towards their equilibrium separation at $T = 0$. Figure 4 shows that the pseudoelastic deformation leads to a much quicker energy release than fully elastic contact formation (especially during the early stages of contact formation). Thus, the pseudoelastic jump to contact represents the preferred path for contact development of two nanoparticles (We note that the total energy change, at the end of the process, corresponds to the change in sum of the surface and interface energies, as we discuss in Sec. II in [21]). Since dislocations are high energy linear crystal defects that typically require extremely large stresses to nucleate in a perfect crystal (shear stresses exceeding 10% of the shear modulus), it is remarkable and counter-intuitive that the nucleation of short-living dislocations in the contact zone represents the most energy efficient adhesive contact formation mechanism for faceted nanoparticles.

The pseudoelastic mechanism of adhesive contact formation is similar to the recently discovered shape memory and superelasticity effects in metallic nanowires [27, 28]. While in classical superelasticity, large elastic strains are absorbed by martensitic twins, in the case of the local deformation observed here, the large elastic strains are reversibly absorbed by dislocations (and their accompanying stacking faults). In full analogy with twinning and superelasticity in nanowires [27], these defects escape from the particles after the contact is formed, leaving a defect-free material. Our results demonstrate that exceeding the yield strength of the material in the contact zone may lead to plastic deformation but does not imply that any dislocation debris will be left behind in the particles. The whole process is terminated in a few picoseconds, making the rapid dislocation-mediated

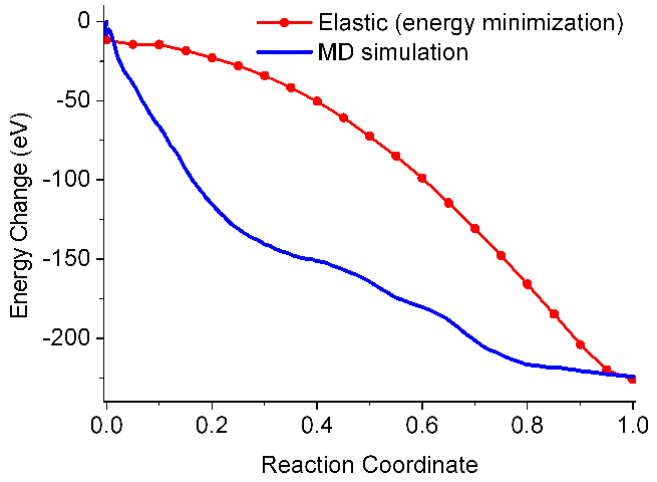

FIG. 4: (Color online) The change in the total energy of the system during adhesive contact formation of two identical 5.7 nm nanoparticles. The reaction coordinate is $(d_0 - d)/(d_0 - d_f)$, where d, d_0 and d_f are the instantaneous separations between the nanoparticle centres, at the separation below which there is interaction between the particles and when the particles are in final contact.

deformation mechanism faster than competing processes such as surface diffusion as proposed to describe contact formation between a gold AFM tip and a gold nanoparticle [29]. Moreover, our MD simulations (not reported here) show that if the surface is not atomically-flat (e.g., an AFM tip approaches a surface with nanosized roughness), the atomic steps serve as hot spots for dislocation nucleation, which may results in *permanent* plastic deformation during contact. These dislocations nucleated during contact formation may be important during friction as well [30].

To summarize, we provide explicit evidence for dislocation-mediated pseudoelastic adhesive contact at the nanoscale. The dislocations relieve the high local stresses that occur during jump-to-contact. These dislocations are not retained in the adhered nanoparticles, which are dislocation-free before and after contact is established. This transient dislocation dynamics mechanism represent the favored mechanism for contact formation in metallic nanoscale systems.

I. ACKNOWLEDGMENTS

This work was supported by the US-Israel Bi-National Science Foundation under the grant No. 2006-109. Partial support from the Russell Berry Nanotechnology Institute at the Technion is heartily acknowledged. We thank Dr. D. Shilo and Prof. D. Sherman for valuable discussion.

[1] E. Riedo, F. Lévy, and H. Brune, Phys. Rev. Lett. **88**, 185505 (2002).
[2] V. K. Lazarov, S. A. Chambers, and M. Gajdardziska-Josifovska, Phys. Rev. Lett. **90**, 216108 (2003).
[3] A. Halder and N. Ravishankar, Adv. Mater. **19**, 1854 (2007).
[4] J. R. Groza, *Nanocrystalline powder consolidation methods, in Nanostructured materials: processing, properties and applications* (William Andrew Publishing, Norwich, NY, 2007).
[5] L. Klinger and E. Rabkin, Int. J. Mat. Res. **101**, 75 (2010).
[6] B. Luan and M. O. Robbins, Nature **435**, 929 (2005).
[7] B. Luan and M. O. Robbins, Phys. Rev. E **74**, 026111 (2006).
[8] K. L. Johnson, K. Kendall, and A. D. Roberts, Proc. R. Soc. Lond. A **324**, 301 (1971).
[9] B. V. Derjaguin, V. M. Muller, and Y. P. Toporov, J. Colloid Interface Sci. **53**, 314 (1975).
[10] D. Maugis, J. Colloid Interface Sci. **150**, 243 (1992).
[11] R. A. Alcantar, C. Park, J.-M. Pan, and J. N. Israelachvili, Acta Mater. **51**, 31 (2003).
[12] M. D. Pashley, J. B. Pethica, and D. Tabor, Wear **100**, 7 (1984).
[13] Y. Kadin, Y. Kligerman, and I. Etsion, J. Appl. Phys. **103**, 013513 (2008).
[14] X. Wang, J. Zhuang, Q. Peng, and Y. Li, Nature **437**, 121 (2005).
[15] J. Zhang, Y. Tang, K. Lee, and M. Ouyang, Science **327**, 1634 (2010).
[16] D. Mordehai, M. Kazakevich, D. J. Srolovitz, and E. Rabkin, Acta Mater. **59**, 2309 (2011).
[17] Y. Yao and A. Thölén, Materials Characterizations **44**, 441 (2000).
[18] A. Thölén, J. Mater. Sci **41**, 4466 (2006).
[19] G. Grochola, S. P. Russo, and I. K. Snook, J. Chem. Phys. **123**, 204719 (2005).
[20] D. Mordehai, S-W. Lee, B. Backes, D. J. Srolovitz, W. D. Nix, and E. Rabkin, Acta Mater. **59**, 5202 (2011).
[21] See supplementary material at http://link.aps.org/supplemental/10.1103/PhysRevLett.***.
[22] S. J. Plimpton, J. Comp. Phys. **117**, 1 (1995).
[23] G. Wulff, Zeitschrift fur Krystallographie und Mineralogie **34**, 449 (1901).
[24] W. J. Huang, R. Sun, J. Tao, L. D. Menard, R. G. Nuzzo, and J. M. Zuo, Nature Mat. **7**, 308 (2008).
[25] E. Rabkin and D. J. Srolovitz, Nano Lett. **7**, 101 (2007).
[26] T. Zhu, J. Li, A. Samanta, A. Leach, and K. Gall, Phys. Rev. Lett. **100**, 025502 (2008).
[27] W. Liang and M. Zhou, Nano Lett. **5**, 2039 (2005).
[28] H. S. Park, K. Gall, and J. A. Zimmerman, Phys. Rev. Lett. **95**, 255504 (2005).
[29] D. Erts, A. Lõhmus, R. Lõhmus, H. Olin, A. V. Pokropivny, L. Ryen, and K. Svensson, Appl. Surf. Sci. **188**, 460 (2002).
[30] V. Kalihari, G. Haugstad, and C. D. Frisbie, Phys. Rev. Lett. **104**, 086102 (2010).